Acta Cryst. (1984). B40, 214–218

The Low-Temperature Phase of Sodium Azide

BY S. R. AGHDAEE* AND A. I. M. RAE

Department of Physics, University of Birmingham, Birmingham B15 2TT, England

(*Received* 1 *September* 1983; *accepted* 3 *January* 1984)

Abstract

The low-temperature phase of sodium azide has been studied at a number of temperatures between 12 and 293 K using a combination of single-crystal and powder X-ray techniques. The structure is monoclinic with space group $C2/m$. The unit cell undergoes a discontinuous shear of 0·5° in the ac plane from the rhombohedral ($R\bar{3}m$) structure at the transition temperature (292·2 K), and this is followed by a continuous change amounting to a total shear of 5·3° at 12 K. The unit-cell dimensions at 12 K are a = 6·1654 (5), b = 3·6350 (3), c = 5·2634 (6) Å, β = 107·543 (5)°, and R_{wp} = 14·7. It is concluded that the transition is of the ferroelastic type and is nearly, but not exactly, second order.

Introduction

Sodium azide crystallizes in the rhombohedral space group $R\bar{3}m$ at high temperatures and undergoes a transition to a low-temperature monoclinic phase at around 290 K (Pringle & Noakes, 1968). The crystal structure of the high-temperature phase has been accurately studied using both X-ray and neutron diffraction data (Stevens & Hope, 1977; Choi & Prince, 1976) and the phase transition has been subject to considerable experimental and theoretical investigation by other techniques (Iqbal, 1973; Simonis & Hathaway, 1974; Jeffrey, 1977; Carling & Westrum, 1976; Raich & Gillis, 1976; Raich & Hüller, 1979), but there is little structural information on the low-temperature phase. The present work was carried out with the aim of determining the monoclinic structure as a function of temperature over a wide temperature range below the transition, paying particular attention to structural changes in the vicinity of the transition temperature.

Experimental

The investigation was carried out using single-crystal X-ray diffraction techniques in the temperature range 160 to 282 K and powder X-ray data in the range 12 to 286 K. Single crystals of sodium azide were grown by slow evaporation of a solution in ethanol. A suitable crystal of approximate dimensions 0·1 × 0·15 × 0·5 mm was enclosed in a thin-walled capillary tube, to prevent sublimation, and rotated about its long axis in a Weissenberg camera. This turned out to be the a axis of the high-temperature rhombohedral cell (referred to hexagonal axes). Using Cu $K\alpha$ radiation, zero- and first-layer data were collected at a number of temperatures between 160 and 282 K, the low temperatures being produced by a stream of cold nitrogen gas. The photographs showed the crystals to be triply twinned, as is expected from the nature of the phase transition (Fig. 1). The intensities of the reflections from each of the three fragments were measured and placed on the same scale by comparison of the intensities of reflections common to two or more fragments. In this way 112 independent reflections were measured, the use of data from more than one fragment resulting in a reasonably even distribution of measured points in reciprocal space, despite the

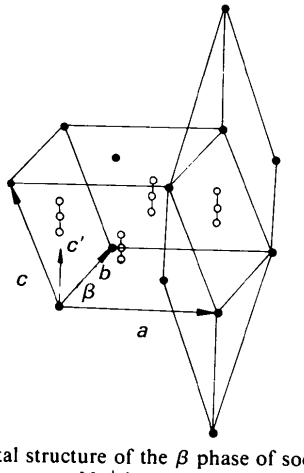

Fig. 1. The crystal structure of the β phase of sodium azide. The filled circles represent Na^+ ions and the triplets of open circles azide ions. The structure is shown referred to both rhombohedral and monoclinic unit cells: in the low-temperature phase the latter distorts by a shear in the ac plane, and a rotation of the azide ions about axes parallel to b. It follows from the rhombohedral symmetry that the structural phase change can occur in any one of three equivalent directions, leading to a triple twinning of the crystals in the low-temperature phase. Understanding of the phase transition is assisted by referring the monoclinic structure to a non-reduced cell of dimensions a, b and c' where, in the high-temperature phase, c' is perpendicular to the ab plane and has magnitude $3c \sin\beta$ (*cf.* Table 1).

* Present address: Department of Physics, University of Science and Technology, Narmak, Tehran, Iran.

0108-7681/84/030214-05$01.50

Table 1. *The cell constants of sodium azide from single-crystal data*

T(K)	a(Å)	b(Å)	c(Å)	β(°)	c'(Å)*	β'(°)*	e_{13}	$e_{22}-e_{11}$
160	6·2233 (42)	3·6510 (27)	5·3359 (25)	108·444 (37)	15·230 (20)	85·636 (10)	0·03816 (9)	0·0161 (12)
210	6·2467 (40)	3·6573 (25)	5·3642 (25)	109·092 (40)	15·239 (20)	86·301 (9)	0·03232 (8)	0·0141 (12)
228	6·2614 (58)	3·6579 (39)	5·3842 (25)	109·522 (55)	15·248 (27)	86·752 (10)	0·02837 (9)	0·0119 (17)
253	6·2764 (31)	3·6558 (25)	5·4178 (16)	110·108 (23)	15·278 (13)	87·417 (3)	0·02256 (3)	0·0088 (9)
272	6·3043 (40)	3·6613 (35)	5·4285 (27)	110·802 (37)	15·233 (19)	88·041 (4)	0·01710 (3)	0·0059 (12)
280	6·3016 (43)	3·6566 (43)	5·4265 (29)	111·106 (35)	15·194 (19)	88·343 (3)	0·01446 (3)	0·0050 (14)
282	6·3105 (40)	3·6578 (20)	5·4830 (20)	111·212 (30)	15·339 (16)	88·658 (2)	0·01171 (2)	0·0039 (11)
295	6·3264 (48)	3·6525 (28)	5·4902 (41)	112·593 (43)	15·206 (23)	90	0	0

* The quantities c' and β' refer to a non-reduced cell that is rectangular ($\beta'=90°$) in the high-temperature phase: $c'=(a^2+9c^2+6ac\cos\beta)^{1/2}$; $\beta'=\cot^{-1}[\cot\beta+(a/3c\sin\beta)]$ (see Fig. 1). The low-temperature cell is obtained from the high-temperature cell by applying the strains e_{13} and $e_{22}-e_{11}$ where $e_{13}=\frac{1}{2}\cot\beta'$ and $e_{22}-e_{11}=(\sqrt{3}b-a)/a$.

Table 2. *The final results of the single-crystal structure refinement*

T(K)		x	z	B_{11}(Å^2)	B_{22}(Å^2)	B_{33}(Å^2)	B_{13}(Å^2)	B_{iso}(Å^2)	θ(°)	R
160	Na	0	0	0·8 (2)	1·2 (2)	0·1 (2)	−0·2 (2)	0·7 (1)	9·40 (21)	0·09
	N(2)	0	0·5	2·3 (6)	0·6 (6)	2·4 (6)	0·7 (5)	1·9 (2)		
	N(1)	0·0939 (19)	0·7313 (21)	3·1 (5)	2·1 (5)	3·1 (5)	1·0 (4)	2·9 (2)		
210	Na	0	0	1·0 (2)	1·7 (3)	0·2 (2)	−0·2 (1)	0·9 (1)	9·03 (19)	0·09
	N(2)	0	0·5	2·4 (6)	1·1 (6)	3·0 (6)	0·8 (5)	2·3 (2)		
	N(1)	0·0951 (18)	0·7320 (21)	2·9 (5)	2·8 (6)	3·0 (5)	0·7 (4)	3·1 (2)		
228	Na	0	0	1·6 (2)	1·7 (2)	0·7 (2)	0·0 (1)	1·4 (1)	7·78 (14)	0·08
	N(2)	0	0·5	2·3 (5)	1·3 (5)	3·3 (6)	0·8 (4)	2·4 (2)		
	N(1)	0·0914 (15)	0·7297 (18)	3·4 (4)	3·5 (6)	3·7 (4)	0·9 (4)	3·8 (2)		
253	Na	0	0	1·4 (2)	1·5 (3)	0·6 (2)	0·1 (2)	0·1 (1)	5·77 (14)	0·09
	N(2)	0	0·5	2·4 (6)	1·8 (6)	3·1 (6)	1·1 (5)	2·5 (3)		
	N(1)	0·0882 (19)	0·7329 (23)	3·8 (5)	3·2 (6)	4·4 (5)	1·5 (5)	3·8 (3)		
272	Na	0	0	1·6 (4)	1·8 (7)	1·3 (4)	0·0 (3)	1·6 (2)	4·72 (20)	0·10
	N(2)	0	0·5	3·1 (9)	1·0 (8)	3·0 (10)	1·3 (9)	2·6 (5)		
	N(1)	0·0854 (34)	0·7294 (33)	4·5 (9)	2·0 (10)	3·5 (9)	0·9 (7)	3·7 (5)		
280	Na	0	0	1·3 (4)	2·0 (7)	0·5 (3)	0·1 (3)	1·1 (2)	4·32 (18)	0·11
	N(2)	0	0·5	3·0 (10)	0·0 (10)	3·5 (9)	1·0 (9)	2·6 (5)		
	N(1)	0·0855 (34)	0·7306 (35)	4·0 (10)	2·0 (1)	4·0 (9)	1·1 (8)	3·7 (5)		
282	Na	0	0	2·1 (3)	3·2 (6)	2·0 (3)	0·4 (3)	2·0 (3)	3·53 (11)	0·08
	N(2)	0	0·5	1·7 (6)	3·0 (10)	1·9 (6)	0·8 (5)	1·6 (6)		
	N(1)	0·0836 (20)	0·7295 (21)	3·0 (6)	3·9 (8)	3·0 (5)	1·1 (4)	2·8 (6)		

fact that only two layers of data were collected. The intensities were corrected for Lorentz and polarization factors, but no allowance was made for absorption.

Powder specimens of sodium azide were mounted in a flat specimen holder which was cooled by conduction to a reservoir of liquid nitrogen and whose temperature could be adjusted by means of a heater (Young, 1966). This apparatus was placed on a Picker X-ray powder diffractometer and, using monochromated Cu $K\alpha_1$ X radiation ($\lambda=1{\cdot}54056$ Å), intensity data were collected by the step-scan method over the 2θ range 16 to 100° using a step length of $\frac{1}{15}$ or $\frac{1}{30}$°, depending on the time available, and an exposure time of 20 or 30 s.

Structure refinement

(i) *Single-crystal data*

The unit-cell dimensions were obtained from the single-crystal data by least-squares refinement using values of the Bragg angles of the *h*0*l* and *hhl* reflections measured in the zero-layer Weissenberg photograph. No corrections were made for systematic errors and the results are given in Table 1 along with their calculated standard deviations.

The only positional parameters not fixed by symmetry are the x and z coordinates of the end atom of the azide ion. These were refined along with anisotropic temperature factors for each atom and an overall scale factor using the *SHELX*76 (Sheldrick, 1976) computer package. The Na^+ scattering factor was that of Cromer & Mann (1968) while those for the central and end N atoms in the azide ion were as determined by Stevens & Hope (1977) from a fit of spherical charge distributions to the calculated molecular electron density of an azide ion. Unit weights were used. The final values of the parameters and the corresponding R factors (defined as $\sum||F_o|-|F_c||/\sum|F_o|$) are given in Table 2.

At temperatures very close to the transition, most of the twinned reflections could not be resolved so a full analysis of the structure was not possible. However, it was clear from the lower-temperature results that the unit-cell changes associated with the phase transition are primarily a shear strain (e_{13}) in the *ac* plane along with a strain ($e_{22}-e_{11}$)= $(\sqrt{3}b-a)/a$ which removes the rhombohedral relation $a=\sqrt{3}b$. If it is assumed that other relevant functions of the cell dimensions are independent of temperature, the two strains can be calculated from the Bragg-angle splittings between the twin components of two reflections. Accordingly, an experi-

Table 3. *The strain components relating the low-temperature to the high-temperature structure as measured from the splitting of high-angle reflections*

T(K)	$\theta_{60\bar{6}} - \theta_{333}$ (°)	$\theta_{33\bar{5}} - \theta_{602}$ (°)	e_{13}	$e_{22} - e_{11}$
288·2	2·94	2·16	0·0101	0·0050
288·6	2·86	2·07	0·0097	0·0051
289·0	2·80	2·00	0·0096	0·0051
289·4	2·75	1·95	0·0093	0·0051
289·8	2·55	1·82	0·0087	0·0047
290·2	2·52	1·82	0·0087	0·0044
290·6	2·31	1·58	0·0077	0·0047
291·0	2·23	1·53	0·0075	0·0045
291·4	2·12	1·45	0·0071	0·0043
291·8	1·70	1·34	0·0061	0·0023
292·2	1·20	1·01	0·0041	0·0012
>292·2	0	0	0	0

The strain components were calculated from the splittings ($\delta\theta$) between lines of Miller indices $h_1k_1l_1$ and $h_2k_2l_2$ where

$$\sin \delta\theta = [(h_2^2 - h_1^2)A(e_{22} - e_{11}) - (h_2l_2' - h_1l_1')Be_{13}]\lambda^2/4 \sin 2\theta.$$

θ is the average value of the Bragg angle and is effectively constant over the temperature range as are the quantities A and B which are given by

$$A = (\sqrt{3}b + a \sin \beta')/(3a^2b^2 \sin \beta') \text{ and } B = 4/ac' \sin \beta'.$$

c' and β' are defined in the note to Table 1 and $l' = 3l + h$.

ment was set up in which the high-angle reflection pairs ($60\bar{6}$; 333) and (602; $33\bar{5}$) were recorded in a small oscillation range; the temperature was changed, the Weissenberg camera was translated a short distance and another exposure was made. In this way the splittings were recorded at temperature intervals of 0·4 K between 288·2 and 293·0 K. The results are set out in Table 3 and Fig. 2.*

(ii) *Powder data*

The powder data were refined by profile refinement (Rietveld, 1969) using the program of Wiles & Young (1981). The flat specimen geometry gives rise to absorption corrections to the peak positions and intensities, and the program was modified to allow for these, assuming a very thick specimen and using the formulae of Langford & Wilson (1962). The peak-shape function used was a modified Lorentzian of the form $P(2\theta) = (0{\cdot}8194/H)[1 + 1{\cdot}6569(2\theta - 2\theta_o)^2/H^2]^{1/2}$, where $2\theta_o$ is the peak position and H is the half width. The unit-cell dimensions, atomic coordinates and isotropic temperature factors were refined along with an overall scale factor, the zero error in 2θ, the standard u, v, w parameters describing the angular dependence of the half width, and the background, represented as a fifth-order polynomial in 2θ. The final values of the structural parameters are given in Table 4 and Fig. 3 shows the final observed and calculated profiles at 82 K. The corresponding profiles at other temperatures are quite similar to this one.*

Results and discussion

The final results of the refinements along with their estimated standard deviations are set out in the tables. The standard deviations almost certainly underestimate the precision of some of the results for a number of reasons. Because of the design of the specimen holder, it was not possible to centre the powder specimen by the standard method of bisecting the straight-through X-ray beam, and a comparatively imprecise method based on adjusting for maximum Bragg intensity had to be used. The resulting centring errors change the apparent peak positions by an amount that is proportional to $\cos\theta$ and, given that the useful data span the 2θ range 30 to 100°, this gives rise to a scan-zero error and a systematic error in the apparent cell size. This effect is particularly noticeable in the two refinements at 179 K where the two sets of linear cell dimensions are related by a factor of 1·0035 and the scan zeros differ by nearly half a degree. As the scan-zero error associated with the first

* Lists of structure factors (single-crystal data) and powder data at the various temperatures have been deposited with the British Library Lending Division as Supplementary Publication No. SUP 39118 (36 pp.). Copies may be obtained through The Executive Secretary, International Union of Crystallography, 5 Abbey Square, Chester CH1 2HU, England.

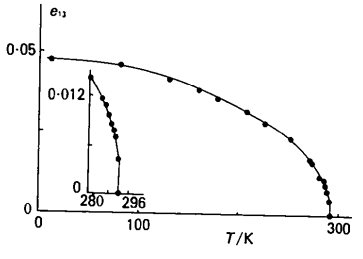

Fig. 2. The temperature dependence of the shear strain e_{13}. The lines are guides to the eye.

* See deposition footnote.

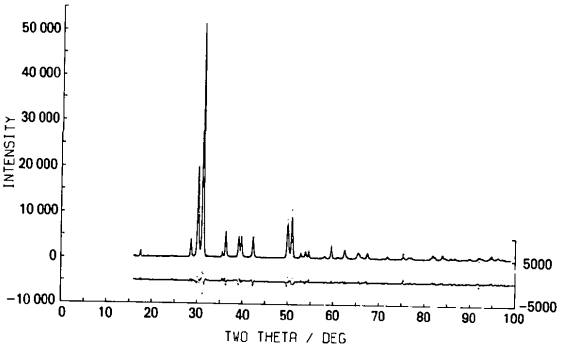

Fig. 3. The powder data at 82 K. The upper curve compares the final calculated profile with the observed data points and the lower curve shows the difference between the observed and calculated profiles.

Table 4. *The final results of structure refinement at different temperatures using the Rietveld method*

T(K)	a(Å)	b(Å)	c(Å)	β(°)	e_{13}	$e_{22}-e_{11}$	x[N(1)]
12	6·1654 (5)	3·6350 (3)	5·2634 (6)	107·543 (5)	0·0467 (1)	0·0212 (1)	0·0984 (3)
82 1	6·1898 (5)	3·6448 (3)	5·2907 (5)	107·735 (4)	0·0447 (1)	0·0199 (1)	0·0992 (3)
82 2	6·1823 (6)	3·6429 (4)	5·2868 (6)	107·777 (6)	0·0443 (1)	0·0206 (2)	0·0980 (4)
130 1	6·1972 (4)	3·6429 (3)	5·3015 (4)	108·165 (4)	0·0410 (1)	0·0182 (1)	0·0961 (3)
130 2	6·1970 (6)	3·6435 (4)	5·3006 (6)	108·168 (6)	0·0410 (1)	0·0184 (2)	0·0972 (4)
179 1	6·2013 (6)	3·6352 (4)	5·3114 (6)	108·823 (5)	0·0352 (1)	0·0153 (2)	0·0951 (3)
179 2	6·2218 (6)	3·6485 (4)	5·3295 (6)	108·789 (5)	0·0354 (1)	0·0156 (2)	0·0935 (3)
227	6·2520 (5)	3·6543 (3)	5·3647 (5)	109·584 (5)	0·0283 (1)	0·0121 (1)	0·0909 (4)
275	6·2971 (5)	3·6593 (3)	5·4369 (6)	110·832 (5)	0·0163 (1)	0·0065 (1)	0·0883 (4)
286	6·2850 (12)	3·6436 (7)	5·4379 (14)	111·396 (11)	0·0111 (3)	0·0041 (3)	0·0786 (8)

	z[N(1)]	θ(°)	B(Na)(Å^2)	B[N(2)](Å^2)	B[N(1)](Å^2)	Scan zero(°)	R_{wp}*
12	0·7271 (4)	12·20 (5)	1·01 (6)	1·31 (11)	0·81 (8)	−0·111 (3)	14·7
82 1	0·7300 (4)	11·85 (4)	1·77 (5)	0·52 (9)	2·26 (7)	−0·170 (2)	20·5
82 2	0·7278 (5)	11·75 (5)	1·82 (7)	1·26 (13)	1·77 (9)	−0·078 (3)	17·4
130 1	0·7283 (3)	10·74 (4)	1·64 (3)	0·59 (9)	1·37 (7)	−0·186 (2)	19·7
130 2	0·7270 (4)	11·23 (5)	2·09 (6)	1·19 (12)	1·97 (9)	−0·040 (3)	16·9
179 1	0·7249 (4)	10·24 (4)	2·11 (7)	1·14 (12)	1·53 (8)	−0·405 (3)	22·8
179 2	0·7263 (4)	9·61 (4)	1·69 (7)	0·92 (11)	1·77 (8)	0·044 (3)	16·2
227	0·7293 (4)	7·68 (3)	3·04 (6)	2·26 (11)	3·33 (7)	−0·204 (2)	19·7
275	0·7380 (4)	4·53(2)	5·88 (8)	1·96 (12)	5·60 (9)	−0·197 (1)	21·8
286	0·7201 (9)	2·95 (3)	3·12 (9)	2·50 (16)	2·23 (11)	−0·108 (6)	20·7

* $R_{wp} = 100 \times \{\sum w_i[y_i(\text{obs.}) - y_i(\text{calc.})]^2 / \sum w_i y_i^2(\text{obs.})\}^{1/2}$.

data set at 179 K is the largest of all those recorded it can be confidently concluded that the precision of the linear cell dimensions obtained from the powder refinement is better than 0·4%, and it is also noted that the powder and single-crystal results are in agreement to about this accuracy. Centring errors have a much weaker effect on parameters that are a function of cell shape rather than overall size and, as a result, independent measurements of the strains e_{13} and $(e_{22}-e_{11})$ generally agree within the estimated standard deviations.

Turning to the structural parameters (in particular the atomic positions and temperature factors) it is well known that their precision is correctly estimated by the calculated standard deviation only if there are no systematic errors in the model. However, it is clear from the final powder profile (Fig. 3) that there are residual model errors which are probably primarily associated with inadequacies in the peak-shape function: a more detailed study of the data shows that there is an anisotropic variation of peak widths in reciprocal space, the 00l peaks being significantly narrower than others at similar Bragg angles. The significance of such model errors has been the subject of much discussion (*e.g.* Sakata & Cooper, 1979; Pawley, 1980; Prince, 1981; Scott, 1983) and there is no generally agreed method for assessing the precision in such circumstances. In the present case, a comparison of the results of different powder runs at the same temperature and a comparison between the powder and single-crystal results indicate that the errors in the powder parameters are probably of the same order as the estimated standard deviations in the single-crystal case and are therefore around five times larger than the standard deviations estimated in the powder refinement. It is noted that the application of the procedure suggested by Pawley (1980) (where the precision is estimated by calculating a standard deviation in the usual way, but with the data-point number reduced by a factor equal to the number of data points contained in the full width at half height of a typical peak) leads to estimated errors about four times the calculated standard deviations.

The phase transition is typified by the two strains e_{13} and $(e_{22}-e_{11})$ along with the angle θ through which the azide ion is rotated from its symmetric orientation parallel to the c axis. Tables 1 to 4 show these quantities as functions of temperature and it is seen that, within experimental error, they are mutually proportional throughout the temperature range. Their temperature variation is therefore typified by that of the strain e_{13} which is shown in Fig. 2. Of particular interest is the behaviour at 292·2 K where the strain undergoes a small discontinuity, below which temperature it increases continuously. It is concluded that the transition temperature is 292·2 K, that the phase transition is of the ferroelastic type where one or more strain components form the order parameter (Wadhawan, 1983) and that it is nearly, but not quite, second order. A detailed theoretical analysis of the transition, using the data reported here and those from other relevant experiments, has been carried out and is reported elsewhere (Aghdaee & Rae, 1983).

The authors gratefully acknowledge advice and assistance obtained from Dr J. I. Langford and Mr R. Pflaumer.

References

AGHDAEE, S. R. & RAE, A. I. M. (1983). *J. Chem. Phys.* **49**, 4558.
CARLING, R. W. & WESTRUM, F. F. (1976). *J. Chem. Thermodyn.* **8**, 565–573.
CHOI, C. S. & PRINCE, E. (1976). *J. Chem. Phys.* **64**, 4510–4516.
CROMER, D. T. & MANN, J. B. (1968). *Acta Cryst.* A**24**, 321–324.
IQBAL, Z. (1973). *J. Chem. Phys.* **59**, 1769–1774.
JEFFREY, K. R. (1977). *J. Chem. Phys.* **66**, 4677–4682.
LANGFORD, J. I. & WILSON, A. J. C. (1962). *J. Sci. Instrum.* **39**, 581–585.
PAWLEY, G. S. (1980). *J. Appl. Cryst.* **13**, 630–633.
PRINCE, E. (1981). *J. Appl. Cryst.* **14**, 157–159.
PRINGLE, G. E. & NOAKES, D. E. (1968). *Acta Cryst.* B**24**, 262–269.
RAICH, J. C. & GILLIS, W. S. (1976). *J. Chem. Phys.* **65**, 2088–2094.
RAICH, J. C. & HÜLLER, A. (1979). *J. Chem. Phys.* **70**, 3669–3672.
RIETVELD, H. M. (1969). *J. Appl. Cryst.* **2**, 65–71.
SAKATA, M. & COOPER, M. J. (1979). *J. Appl. Cryst.* **12**, 554–563.
SCOTT, H. G. (1983). *J. Appl. Cryst.* **16**, 159–163.
SHELDRICK, G. M. (1976). *SHELX*76. A program for crystal structure determination. Univ. of Cambridge, England.
SIMONIS, G. J. & HATHAWAY, C. E. (1974). *Phys. Rev. B*, **10**, 4419–4433.
STEVENS, E. D. & HOPE, H. (1977). *Acta Cryst.* A**33**, 723–729.
WADHAWAN, V. K. (1983). *Phase Transitions*, **3**, 3.
WILES, D. B. & YOUNG, R. A. (1981). *J. Appl. Cryst.* **14**, 149–151.
YOUNG, R. A. (1966). *J. Sci. Instrum.* **43**, 449–453.

Acta Cryst. (1984). B**40**, 218–222

Synthetic Epsomite, $MgSO_4.7H_2O$: Absolute Configuration and Surface Features of the Complementary {111} Forms

BY M. CALLERI, A. GAVETTI, G. IVALDI AND M. RUBBO

Istituto di Mineralogia, Cristallografia e Geochimica dell'Università, Via San Massimo 22, 10123 *Torino, Italy*

(*Received* 17 *October* 1983; *accepted* 10 *January* 1984)

Abstract

Epsomite, $MgSO_4.7H_2O$, $M_r = 246{\cdot}5$, is orthorhombic, space group $P2_12_12_1$. To establish its absolute configuration, a slab was cut from a laevorotatory crystal, grown under controlled conditions, and used for diffractometer measurements with graphite-monochromatized Cu $K\alpha$ radiation ($\lambda = 1{\cdot}54178$ Å): $a = 11{\cdot}876$ (2), $b = 12{\cdot}002$ (2), $c = 6{\cdot}859$ (1) Å (parameters obtained and refined from 17 reflexions, $87° \leq 2\theta \leq 113°$), $V = 977{\cdot}7$ (2) Å^3, $Z = 4$, $F(000) = 520$, $D_x = 1{\cdot}67$ Mg m^{-3}, μ(Cu $K\alpha$) = 4·01 mm^{-1}, room temperature. Refinement based on 1602 reflexions, 1292 of which were Friedel pairs. Final R for the correct and incorrect enantiomorphs were 0·0797 and 0·0836 respectively, which, taken with the relative F_o, F_c values of the Friedel pairs and with the results from a test proposed by Rogers [*Acta Cryst.* (1981), A**37**, 734–741], allow the correct configuration to be assigned at a very high confidence level. To have an accurate, room-temperature, determination, a second refinement was completed with a second crystal and graphite-monochromatized Mo $K\alpha$ radiation (λ = 0·71069 Å): $a = 11{\cdot}887$ (2), $b = 12{\cdot}013$ (2), $c = 6{\cdot}861$ (1) Å (parameters from 25 reflexions, $23° \leq 2\theta \leq 55°$), $V = 979{\cdot}8$ (1) Å^3, $D_x = 1{\cdot}67$ Mg m^{-3}, μ(Mo $K\alpha$) = 0·42 mm^{-1}. R for the correct and incorrect configurations 0·0300, 0·0307 for 2848 independent reflexions. The absolute configuration has been correlated with crystal morphology and the relative growth rates of the complementary {111} and $\{\bar{1}\bar{1}\bar{1}\}$ forms within the field of low supersaturations. The surface features account for the predominance of $\{\bar{1}\bar{1}\bar{1}\}$.

Introduction

One of the problems to be faced when studying the growth from solution of noncentrosymmetric crystals is the determination of the difference $(\Delta P_{hkl} - \Delta P_{\bar{h}\bar{k}\bar{l}})$, where ΔP stands for the variation of P (polarization energy of the crystal surfaces hkl, $\bar{h}\bar{k}\bar{l}$) due to the adsorption of crystal building units coming from the mother phase. ΔP is strictly related to the surface of the crystal faces and, therefore, in the case of noncentrosymmetric crystals, $\Delta P_{hkl} \neq \Delta P_{\bar{h}\bar{k}\bar{l}}$. ΔP does influence the orthogonal-growth rate (R_{hkl}) of a given form. The mean free-path of a building unit on an (hkl) face, x^s_{hkl}, is a function of the total activation energy for the surface diffusion $\Delta G_{s.diff.} = U_s + \Delta P$, U_s being the activation energy for a building unit to diffuse between two adjacent and equivalent surface sites assumed as undeformed, that is as if they belonged to the crystal bulk structure. Monier & Kern's (1956, and references therein) theory leads to the following growth-rate ratio for two complementary forms, within the field of low supersaturation values:

$$\frac{R_{hkl}}{R_{\bar{h}\bar{k}\bar{l}}} = \frac{x^s_{hkl}}{x^s_{\bar{h}\bar{k}\bar{l}}} = \exp\left(-\frac{\Delta P_{hkl} - \Delta P_{\bar{h}\bar{k}\bar{l}}}{2kT}\right). \quad (1)$$

Equation (1) implies that when $\Delta P_{hkl} > \Delta P_{\bar{h}\bar{k}\bar{l}}$, $x^s_{hkl} < x^s_{\bar{h}\bar{k}\bar{l}}$, that is, to a greater polarization of one form corresponds a shorter mean free-path, and therefore

0108-7681/84/030218-05$01.50